Chinese Journal of
POLYMER SCIENCE

ARTICLE

https://doi.org/10.1007/s10118-018-2138-3
Chinese J. Polym. Sci. 2018, 36, 1175–1186

Preparation of Polylactide/Poly(ether)urethane Blends with Excellent Electro-actuated Shape Memory *via* Incorporating Carbon Black and Carbon Nanotubes Hybrids Fillers

Yuan Wei, Rui Huang, Peng Dong, Xiao-Dong Qi*, and Qiang Fu*

College of Polymer Science and Engineering, State Key Laboratory of Polymer Materials Engineering, Sichuan University, Chengdu 610065, China

Abstract In this work, hybrid conductive fillers of carbon black (CB) and carbon nanotubes (CNTs) were introduced into polylactide (PLA)/thermoplastic poly(ether)urethane (TPU) blend (70/30 by weight) to tune the phase morphology and realize rapid electrically actuated shape memory effect (SME). Particularly, the dispersion of conductive fillers, the phase morphology, the electrical conductivities and the shape memory properties of the composites containing CB or CB/CNTs were comparatively investigated. The results suggested that both CB and CNTs were selectively localized in TPU phase, and induced the morphological change from the sea-island structure to the co-continuous structure. The presence of CNTs resulted in a denser CB/CNTs network, which enhanced the continuity of TPU phase. Because the formed continuous TPU phase provided stronger recovery driving force, the PLA/TPU/CB/CNTs composites showed better shape recovery properties compared with the PLA/TPU/CB composites at the same CB content. Moreover, the CB and CNTs exerted a synergistic effect on enhancing the electrical conductivities of the composites. As a result, the prepared composites exhibited excellent electrically actuated SME and the shape recovery speed was also greatly enhanced. This work demonstrated a promising strategy to achieve rapid electrically actuated SME *via* the addition of hybrid nanoparticles with self-networking ability in binary PLA/TPU blends over a much larger composition range.

Keywords Polymer composites; Shape memory polymer; Co-continuous structure; Self-networking behavior; Hybrid filler

Citation: Wei, Y.; Huang, R.; Dong, P.; Qi, X. D.; Fu, Q. Preparation of Polylactide/Poly(ether)urethane Blends with Excellent Electro-actuated Shape Memory *via* Incorporating Carbon Black and Carbon Nanotubes Hybrids Fillers. Chinese J. Polym. Sci. 2018, 36(10), 1175–1186.

INTRODUCTION

As an emerging class of smart polymers, shape memory polymers (SMPs) can be fixed into a temporary shape, and then recover their permanent shapes in the presence of an external stimulus, such as heat, electricity, light, magnetic fields, and solvents[1–4]. The most widely studied SMPs are thermal-triggered SMPs, in which the shape memory behavior is triggered through heating. However, if the heating process is not available or suitable, alternative stimuli are needed to be considered. Electrical stimulus is a relatively easy procedure to achieve and now receives much interest in research and application[5]. Most SMPs are inert to electrical current, thus preventing the SMP from being directly actuated *via* electrically resistive heating. Therefore, a variety of electrically conductive nanoparticles, such as carbon black (CB), carbon nanofibers (CNFs), carbon nanotubes (CNTs), and graphene *etc.*, have been introduced into SMPs[6–14].

Recently, the blending of plastic/elastomer has become a very effective and economic way to fabricate SMPs[15–18]. For plastic/elastomer SMPs, the plastic acts as a switch unit and fixes the temporary shape while the elastomer component provides entropy elasticity to drive material back to the permanent shape[19, 20]. Although it is an economic and simple way to fabricate this type of SMPs, the shape memory properties depend strongly on the phase morphology of polymer blends. According to previous studies, a co-continuous structure is the key to acquire good shape-fixation and shape-recovery abilities[21, 22]. However, the co-continuous structure of plastic/elastomer blends always appears at a narrow weight ratio (near 50:50), which limits the development of plastic/elastomer SMP blend. Thus, it is important to find a way to broaden the composition range of the co-continuous structure, which allows the flexible control of the ratio of plastic/elastomer.

In recent years, the use of nanoparticles with self-networking properties is considered to be an effective way to broaden the composition range of the co-continuous structure in immiscible polymer blends[23–27]. Our previous work reported an electro-actuated SMP of polylactide (PLA)/thermoplastic poly(ether)urethane (TPU) blends *via* CB self-networking induced co-continuous structure[28]. The phase morphology of PLA/TPU blends (70/30 by weight) was

* Corresponding authors: E-mail qxdjianhu@163.com (X.D.Q.)
E-mail qiangfu@scu.edu.cn (Q.F.)

Received December 27, 2017; Accepted March 30, 2018; Published online April 28, 2018

changed from sea-island structure to co-continuous structure with increasing CB content. With such novel co-continuous structure, a superior shape memory property could be achieved because the formed continuous TPU phase provided a strong recovery force. More importantly, CB also provided electrical conductivity which enabled electro-actuation of such blends. However, a high content of CB, namely, above 6 phr (per hundreds of resin) was required to be incorporated into the PLA/TPU blends to realize such electro-actuated shape memory behavior, which is unfavorable for mechanical properties (*e.g.* ductility) and practical processing of composites.

As another category of the carbon allotropes, carbon nanotubes (CNTs) are widely used in enhancing the electrical properties of polymers due to their high aspect ratio and excellent intrinsic electrical conductivity. Therefore, some researches have been done to study the combined effect between CB and CNTs fillers[29, 30]. For example, Ma *et al.* investigated epoxy/CB/CNTs composites and found that a lower percolation threshold can be achieved by using hybrid CB/CNTs fillers[30]. These two carbonic fillers can form co-supporting conductive networks where long fibrous CNTs act as main contributor of electron transport path while CB nanoparticles become connections of CNTs. So far most of works have been done to introduce both CNTs and CB into single polymer matrix, and only a few works are related to polymer blends[31]. Similar to the synergistic effect of hybrid CNTs/CB in single polymer which enhances electrical conductivities, it is reasonable to assume that hybrid CNTs/CB also show the synergistic effect, leading to a dramatically improved conductivity, if they are simultaneously localized in one phase of the immiscible polymer blends.

In this work, we attempted to incorporate CB and CNTs into PLA/TPU blends (70/30 by weight), aiming at enhancing the electrical conductivity of composites with balanced shape memory properties. There were two objects in this work. The first one was to investigate the morphological changes and related effect on the thermal shape memory properties of PLA/TPU blends after adding a small amount of CB and CNTs, and the second one was to further improve the electrical conductivity and electro-actuated shape memory performance of PLA/TPU blends *via* combined effect of CB and CNTs. The obtained SMPs with electro-actuation, balanced mechanical properties and simple fabrication showed potential applications in soft robotics and artificial mussels.

EXPERIMENTAL

Materials

Polylactide (PLA, 4032D, D-isomer content = 1.2%–1.6%, T_g = 65 °C, T_m = 160 °C) was purchased from NatureWorks Co. Ltd., USA, with a density of 1.25 g/cm^3, having the weight-averaged molecular weight (M_w) of 207 kDa and the polydispersity index (PDI) of 1.74. thermoplastic poly(ether)urethane (TPU, WHT-1570), having a density of 1.21 g/cm^3, was purchased from Yantai Wanhua Polyurethane Co. Ltd., China (T_g = −50 °C). Carbon black (CB, Printex-XE2B) was purchased from Degussa Co. Ltd., Germany, with a primary particle diameter of 30 nm. Multi-walled carbon nanotubes (MWCNTs, Nanocyl 7000) were purchased from Nanocyl S.A., Belgium. All materials were dried in a vacuum oven (set at 80 °C) for 48 h before sample preparation and used without any further treatment.

Preparation

Weighed PLA and TPU (PLA/TPU, 70/30 by weight) with different contents of CB (3 phr, 5 phr) and CNTs (0, 0.25 phr, 0.5 phr, 0.75 phr, 1.0 phr, 2.0 phr) were firstly mixed mechanically for 2 min in a beaker. The mixtures were simultaneously added into an internal mixer (XSS-300, Shanghai, China) at 190 °C with a rotation speed of 60 r/min and melt blended for 6 min. The master-batch was further hot pressed into plates *via* a plate vulcanizer (Qingdao, China) at 190 °C under 10 MPa for 6 min. Composites were named as PLA70/TPU30/C*x*/CNT*y*, where *x* and *y* represented the amount of CB and CNTs, respectively. Sample disks for rheological tests were also prepared through the same process, with the diameter of 25.0 mm and thickness of 1.4 mm.

Characterization

Scanning electron microscopy (SEM)

The cryogenically fractured surfaces of samples were observed by a scanning electron microscope (FEI Inspect F, FEI, USA) under accelerating voltage of 10 kV. The samples were cryogenically fractured in liquid nitrogen, and cryo-fractured surfaces were covered with gold through a sputter coater before testing.

Transmission electron microscopy (TEM)

Localization of filler and phase morphologies of samples were further inspected by a transmission electron microscope (Tecnai G^2 F20 S-TWIN, FEI, USA) at an accelerating voltage of 200 kV. Ultra-thin samples (100 nm thickness) were prepared through cryo-ultramicrotomy (Lecia UCT microtome) at −100 °C, then collected onto a copper grid.

Rheological measurements

A rheometer (Gemini 200, Malvern, British) was employed to characterize rheological properties of samples. The strain amplitude was set to 1% to exhibit the linear visco-elastic response and the angular frequency sweep was set between 0.0628 and 628 rad/s. All samples were investigated at temperature of 190 °C protected by nitrogen atmosphere.

Dynamic mechanical analysis (DMA)

Dynamic mechanical analysis measurements were conducted through DMA (Q-800, TA Instrument, USA). Samples tested were cut into rectangular strips and were heated from −80 °C to 100 °C at rate of 3 °C/min at frequency of 1 Hz.

Quantitative shape memory properties of samples were also evaluated by DMA. The force was imposed while the strain was monitored. Samples were cut to rectangular strips before evaluated. Testing procedures were designed as follows. (1) Deforming: Samples were heated to 85 °C at a rate of 10 °C/min and equilibrated for 5 min. Then, a constant force was loaded, and sample was stretched to ε_m. (2) Fixing: Stretched samples were cooled to room temperature at rate of 10 °C/min and equilibrated for 5 min while maintaining the force. (3) The force was removed, and the strain was recorded as ε_f. (4) Recovery: The samples

https://doi.org/10.1007/s10118-018-2138-3

were re-heated to 85 °C at a rate of 10 °C/min and equilibrated for 15 min to fully recover and the remaining strain ε_r was recorded. Shape recovery ratio (R_r) and shape fixing ratio (R_f) were calculated through equations below:

$$R_r = \frac{\varepsilon_m - \varepsilon_r}{\varepsilon_m} \quad (1)$$

$$R_f = \frac{\varepsilon_f}{\varepsilon_m} \quad (2)$$

Electrical properties and electro-actuated shape memory effect tests

Samples were cut to rectangular strips and coated with silver at both ends to eliminate contact resistance. The electrical resistances were evaluated by a picoammeter (Keithley6487, Tektronix, USA), and then converted to electrical conductivity. Samples tested were subjected to constant voltage using DC power (ITHECH IT6700, USA), and the surface temperature in strip center was monitored by a thermocouple. Also, an infrared thermal imager (Ti-26, Fluke, USA) was employed to investigate the surface temperature of tested samples.

Electro-actuated shape memory effect (SME) was measured through the bending experiment. Samples were also cut to rectangular shape and coated with silver on both sides. Sample strips were first immersed in hot water (85 °C) and bended into a "U"-like shape by external force and were rapidly put into liquid nitrogen to fix deformation. Then the external force was removed and the angle between the two sides of the bent sample (θ_d) was recorded. During the recovery, the angle between the two sides of the sample was also recorded as θ_r. The whole procedure was recorded by a digital camera and an infrared imager. Shape recovery ratio (R_r) of tested samples was calculated through the following equation:

$$R_r = \frac{\theta_r - \theta_d}{180° - \theta_d} \quad (3)$$

Mechanical properties

The impact tests were conducted on an impact tester (XJU-5.5, China) at 23 °C. The tensile tests were conducted on a universal test machine (SANS, Shenzhen, China) with a crosshead speed of 50 mm/min at 23 °C. The average values illustrated in this work were obtained from at least five samples. All samples were equilibrated at 23 °C for 12 h before testing.

The tensile tests at high temperature were inspected through DMA. Samples were firstly heated to 85 °C and equilibrated for 5 min, then stretched at rate of 3 N/min until fracture.

RESULTS AND DISCUSSION

Morphology Change of PLA70/TPU30 Blend by Adding CB and CNTs

According to previous studies, the shape memory properties of plastic/elastomer blends depend strongly on the phase morphology[19, 21, 28]. Scanning electron microscopy was firstly employed to investigate the localization of fillers and the impact on phase morphology of the composites, as shown in Fig. 1. PLA70/TPU30 (Fig. 1a) exhibits typical sea-island structure where spherical TPU domains with several micron sizes are uniformly dispersed in the PLA matrix. Interestingly, PLA70/TPU30/CB3 (Fig. 1b) incorporating 3 phr CB results in a special co-continuous structure, where discrete TPU domains are elongated and partly fuse together. This morphological transition of the TPU phase indicates that 3 phr CB tunes PLA70/TPU30 from the typical sea-island structure to a quasi-continuous structure. Further increasing the content of CB to 5 phr, a denser consecutive network structure is formed since more TPU droplets fuse together during melt blending, as shown in Fig. 1(d). On the other hand, in Fig. 1(c), the addition of 1 phr CNTs also results in an increment in continuity of TPU, which suggests that CNTs nanoparticles also facilitate the filler network, as PLA70/TPU30/CB3/CNTs1 shows a more refined TPU phase than PLA70/TPU30/CB3. According to the literature, such morphological evolution of PLA70/TPU30 blends from a sea-island structure to such unique co-continuous structure is mainly attributed to the filler network constructed by self-networking nanoparticles. In other words, the formed filler network drives TPU droplets together during melt blending *via* a strong affinity between fillers and the TPU. It is interesting to find that CNTs-facilitated filler network leads to a more continuous TPU phase. As a result, further increasing the co-continuity of PLA70/TPU30/CB5/CNTs1 is observed in Fig. 1(e).

In order to further clarify such morphological transitions of TPU phase, as well as the distribution of CB and CNTs,

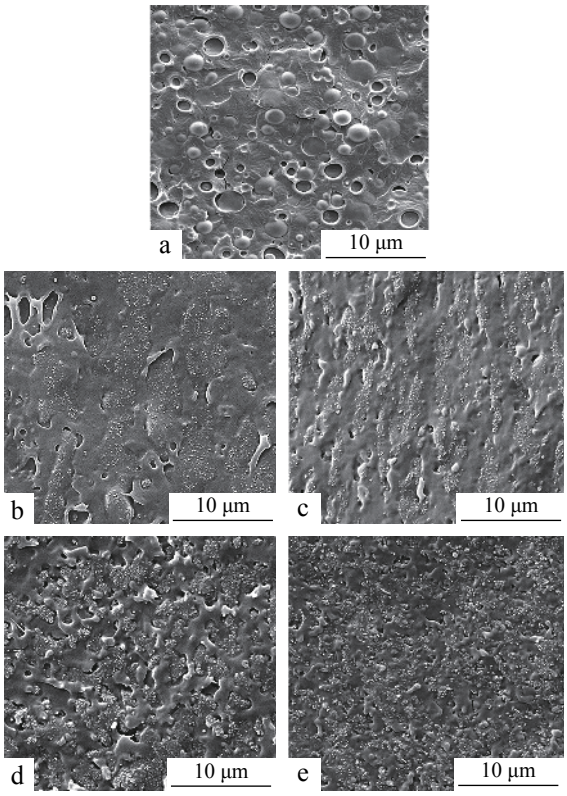

Fig. 1 SEM images of (a) PLA70/TPU30, (b) PLA70/TPU30/CB3, (c) PLA70/TPU30/CB3/CNTs1, (d) PLA70/TPU30/CB5 and (e) PLA70/TPU30/CB5/CNTs1

https://doi.org/10.1007/s10118-018-2138-3

transmission electron microscopy was employed to investigate representative samples, and results are illustrated in Fig. 2. In PLA70/TPU30/CB3 (Fig. 2a), TPU domains (dark parts) are distinctly elongated but still individual, prevailing through PLA matrix (bright parts), and exhibit a quasi-continuous structure. Further raising the content of CB to 5 phr, these isolate TPU domains become more refined and aggregate together, forming a unique co-continuous structure, as shown in Fig. 2(c). Nevertheless, by adding 1 phr CNTs into PLA70/TPU30/CB3, a co-continuous structure is revealed, which also indicates an increment in co-continuity. And a higher continuous degree of TPU phase is observed in PLA70/TPU30/CB5/CNTs1. Interestingly, both CB and CNTs are selectively distributed in the TPU phase, suggesting a strong affinity between TPU phase and fillers.

Literature has reported that the phase morphology of immiscible binary polymer blends can be tuned by the interaction from the polymer and filler networks[32, 33]. Self-networking CB nanoparticles in PLA70/TPU30 blends form a filler network and drive adjacent TPU droplets to aggregate together *via* the strong affinity during melt blending; discrete TPU domains fuse together, forming a co-continuous-like and finally such co-continuous structure of polymer morphology[24, 26]. The incorporation of 3 phr CB tailors PLA70/TPU30 blend into a quasi-continuous structure and 5 phr CB induces a fully co-continuous morphology, because more CB nanoparticles construct a denser filler network, which results in a higher co-continuity. Interestingly, the addition of 1 phr CNTs also leads to the increment in continuity of TPU phase, indicating that CNTs nanoparticles assist a denser filler network. Thus, the morphological evolution of TPU phase suggests that not just CB, the addition of CNTs also increases the continuity of TPU phase. As a result, CNTs also show self-networking ability which can facilitate to forming a dense filler network and improving the co-continuity of PLA70/TPU30 blends.

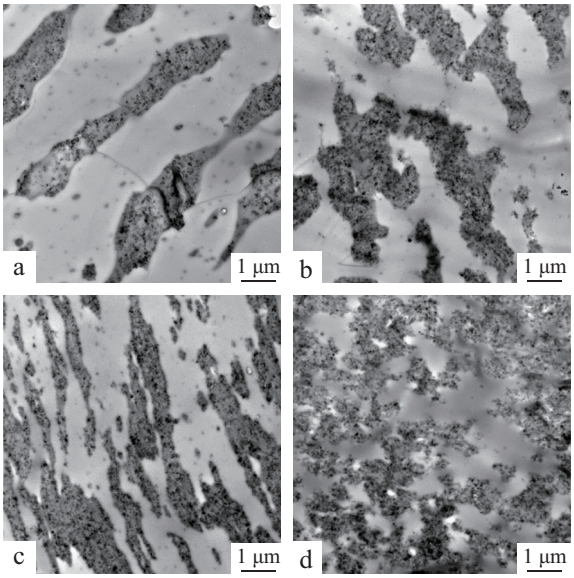

Fig. 2 TEM images of (a) PLA70/TPU30/CB3, (b) PLA70/TPU30/CB3/CNTs1, (c) PLA70/TPU30/CB5, (d) PLA70/TPU30/CB5/CNTs1

The morphological evolution of PLA70/TPU30 blends brought by the filler self-networking can be inspected by a swelling experiment, as shown in Fig. 3. Chloroform is a good solvent for PLA but poor for TPU, and once PLA70/TPU30 blends with a sea-island structure are immersed into chloroform, the whole PLA matrix will be rapidly solved by chloroform, leaving numerous small TPU spheres. However, a continuous TPU scaffold can support the entire polymer matrix. Therefore, PLA70/TPU30/CB3 shows moderately swollen due to the quasi-continuous TPU scaffold while samples with a higher filler content, namely, a higher co-continuity, are only slightly swollen after sunk into chloroform for 12 h.

Rheological measurements are believed to be an efficient way to reveal the filler network in the polymer matrix. Frequency sweep tests of representative samples were conducted. Storage modulus (G') versus angular frequency (ω) curves of representative composites are plotted in Fig. 4. It is widely accepted that a plateau at low frequencies in G'-ω plot indicates a percolated filler network in polymer melt[34]. For PLA70/TPU30, no appearance of plateau is observed in a low frequency range, where discrete TPU domains are uniformly located in the PLA matrix with a sea-island structure and exhibit liquid-like performance. However, in Fig. 4(a), PLA70/TPU30/CB3 shows a plateau in low frequency region, namely, G' becomes independent of the shear frequency. Such transition from a liquid-like to a solid-like viscoelastic performance indicates 3 phr CB have formed a percolated filler network. Moreover, in Fig. 4(b), except exhibiting a plateau in low frequency range, PLA70/TPU30/CB5 shows a higher G' than PLA70/TPU30/CB3. Such improvement in G' indicates the formation of a denser filler network which provides higher restrains to the long-range molecular motion of the polymer matrix. Interestingly,

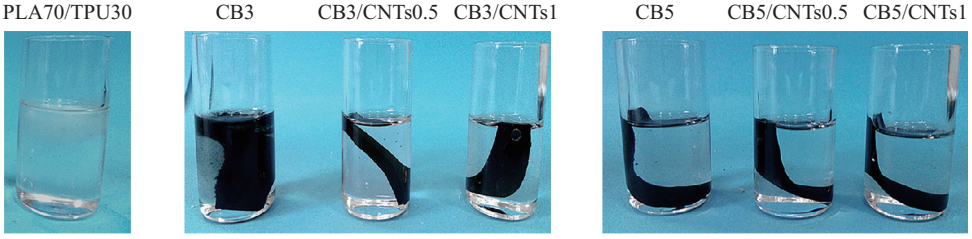

Fig. 3 Photos of swelling experiments for PLA70/TPU30 and PLA70/TPU30/CB/CNTs composites by chloroform (The online version is colorful.)

https://doi.org/10.1007/s10118-018-2138-3

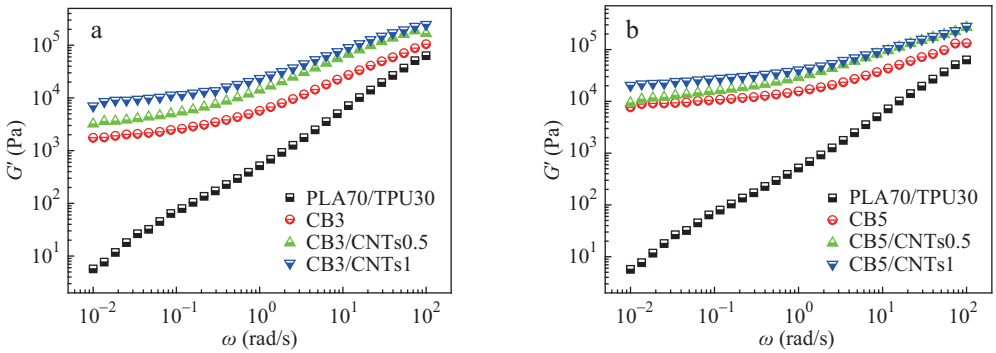

Fig. 4 Frequency dependence of storage modulus (*G*'): (a) PLA70/TPU30/CB3 with varying content of CNTs, (b) PLA70/TPU30/CB5 with varying content of CNTs

the addition of CNTs leads to an increment in *G*', which also suggests the introduced CNTs nanoparticles result in a denser filler network. As discussed above, CNTs nanoparticles are selectively located in TPU. With a denser hybrid filler network and a strong affinity between both filler and TPU domains, a more continuous TPU framework is achieved by such filler network, which is well-matched to SEM and TEM results. However, one should note that, the selectively distributed nanoparticles causes a higher viscosity of TPU while the viscosity of PLA is unchanged. In such case, based on the classical Paule-Barlow theory, the condition of morphological transition from the sea-island structure to the co-continuous structure is shown as:

$$\Phi_1/\Phi_2 = \eta_1/\eta_2$$

where Φ_i and η_i are the volume fraction and melt viscosity of component *i*, respectively. The theory suggests that increasing the volume fraction or decreasing the viscosity of the minor phase would result in a higher continuity in the matrix. In this case, the expected morphology of PLA70/TPU30/CB3/CNTs1 composite should be the sea-island structure rather than the observed co-continuous structure. Therefore, the deviation indicates that the morphological transition is not induced by the change of the viscosity of TPU but the self-networking abilities of introduced nanoparticles.

Shape Memory Properties of PLA70/TPU30/CB/CNTs

Dynamic mechanical tests of the samples were firstly carried out on DMA and the results are shown in Fig. 5. The results reveal two abrupt changes in both storage modulus (*E*') and tanδ of all samples. Note that the larger decrease of *E*' and the increase of tanδ near 65 °C indicate glass transition of PLA matrix in composites. According to the mechanism of plastic/elastomer SMP blends, the plastic provides the shape fixity and keeps the temporary shape *via* crystallization or glass transition. Thus, switch temperature (T_s) was chosen at 85 °C when *E*' of the sample showed a very large decrease to exhibit SME, and deformations could be fixed below T_s of PLA by the glassy domains.

Quantitative shape memory performances were evaluated through dual-SME tests and were conducted on DMA. Each specimen was conducted more than 5 times and repeatable results were obtained, as displayed in Fig. 6. Specimens are uniaxially stretched at T_s and rapidly cooled to room temperature (25 °C) to fix deformation. Then samples are reheated to T_s, where a large strain has recovered while an unrecovered strain remains. All samples present a little recovery of strain after shape fixity. PLA70/TPU30 blend exhibits a much higher unrecovered strain (30%) after shape recovery than PLA70/TPU30/CB3 (12%). Moreover, PLA70/TPU30/CB5 shows a less unrecovered strain (10%) than PLA70/TPU30/CB3 after shape recovery. Interestingly, the addition of 1 phr CNTs further decreases the unrecovered strain, as PLA70/TPU30/CB3/CNTs1 and PLA70/TPU30/CB5/CNTs1 exhibit values less than 10%.

Moreover, quantitative shape memory properties can be described by shape fixing ratio (*Rf*) and shape recovery ratio

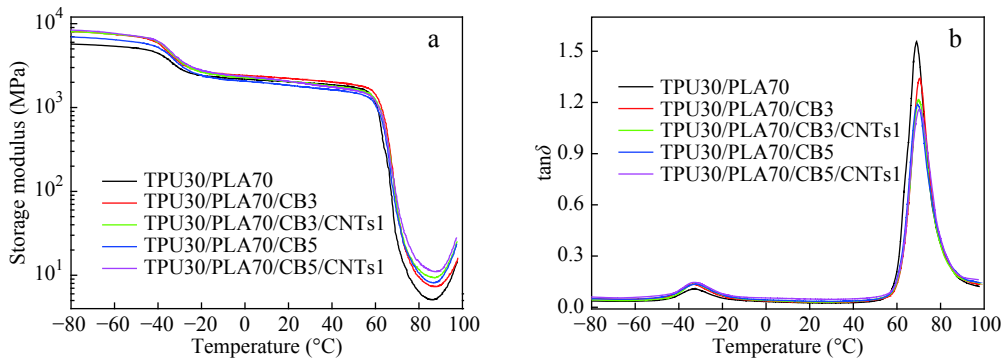

Fig. 5 Dynamic mechanical analysis test of representative PLA70/TPU30/CB/CNTs composites: (a) storage modulus as function of temperature, (b) tangent of dynamic loss angel as function of temperature

https://doi.org/10.1007/s10118-018-2138-3

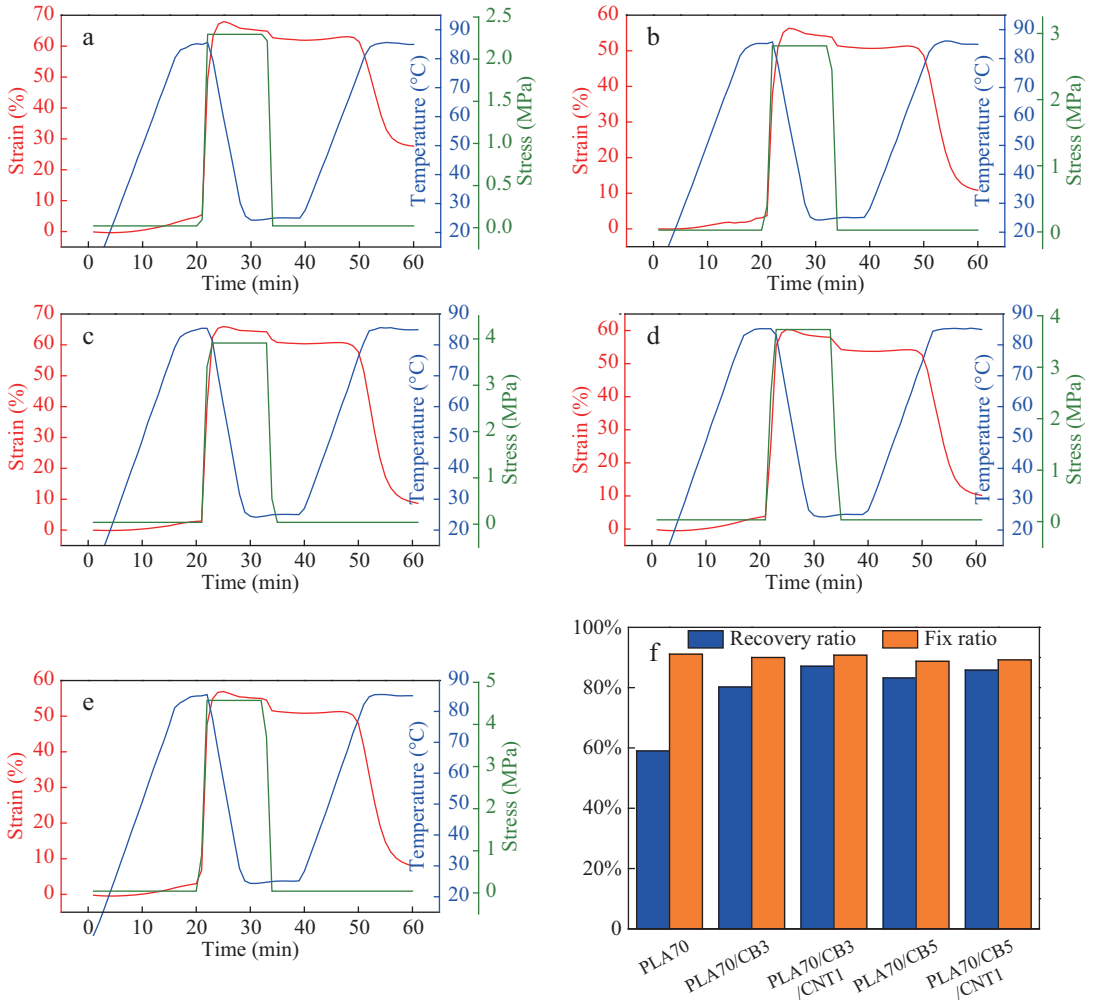

Fig. 6 The thermal-mechanical tensile curves of (a) PLA70/TPU30, (b) PLA70/TPU30/CB3, (c) PLA70/TPU30/CB3/CNTs1, (d) PLA70/TPU30/CB5, and (e) PLA70/TPU30/CB5/CNTs1; (f) Shape fixing ratio (R_f) and shape recovery ratio (R_r) of PLA70/TPU30/CB/CNTs composites

(R_r), which are calculated through Eqs. (1) and (2) and results are plotted in Fig. 6(f). As one can see, all composites have a relatively high R_f (all > 88%), indicating the filler induced morphological evolution of TPU phase impacts little on shape fixity. Nevertheless, R_r presents obviously much more differences, as the PLA70/TPU30 has relatively lower R_r of 59%, while filler enhanced samples show higher R_r (≥ 80%). PLA70/TPU30 composites filled with 3 and 5 phr CB show R_r of 80% and 82%, respectively. Moreover, after addition of 1 phr CNTs, PLA70/TPU30/CB3/CNTs1 exhibits 5% increment in R_r (85%), but PLA70/TPU30/CB5/CNTs1 only increases a little and exhibits a R_r of 83%.

To understand deep inside of the variation in shape fixity and recovery, we propose a possible mechanism of the shape memory properties of PLA70/TPU30/CB/CNTs composites, as shown in Fig. 7. PLA70/TPU30 blends can be easily deformed above T_g of PLA, and amorphous PLA chains are frozen by rapidly cooling down to ambient temperature (25 °C) below its T_g. After releasing the deformation force at room temperature, no instant shrinkage is observed, since the consecutive PLA matrix exhibits a higher modulus than the resilience from the deformed TPU phase. Thus, the temporary shape can be well held. The resilience which drives the strain recovery is mainly originated from stored stress in the deformed TPU phase, which is well restricted by stiffness of the glassy PLA chains at ambient temperature. Hence, all composites show relatively high R_f due to strict restrains from the continuous PLA matrix.

Literature suggests that shape memory behaviors of plastic/elastomer blends are largely dependent on their phase morphology. In this work, hybrid CB/CNTs nanoparticles tune the phase morphology of PLA70/TPU30 from the typical sea-island structure to a unique co-continuous phase. Herein, the morphological evolution of TPU phase is considered to be the main contributor for increment in R_r. For PLA70/TPU30, numerous individual TPU domains are uniformly dispersed in the PLA matrix, exhibiting a typical sea-island structure. The R_r of PLA70/TPU30 is relatively low, since the discrete TPU droplets are unable to provide a strong enough resilience to fully drive the entire matrix back to its permanent shape, as shown in Fig. 7(a). The addition of CB (3 phr) tailors TPU from isolated domains to a quasi-

https://doi.org/10.1007/s10118-018-2138-3

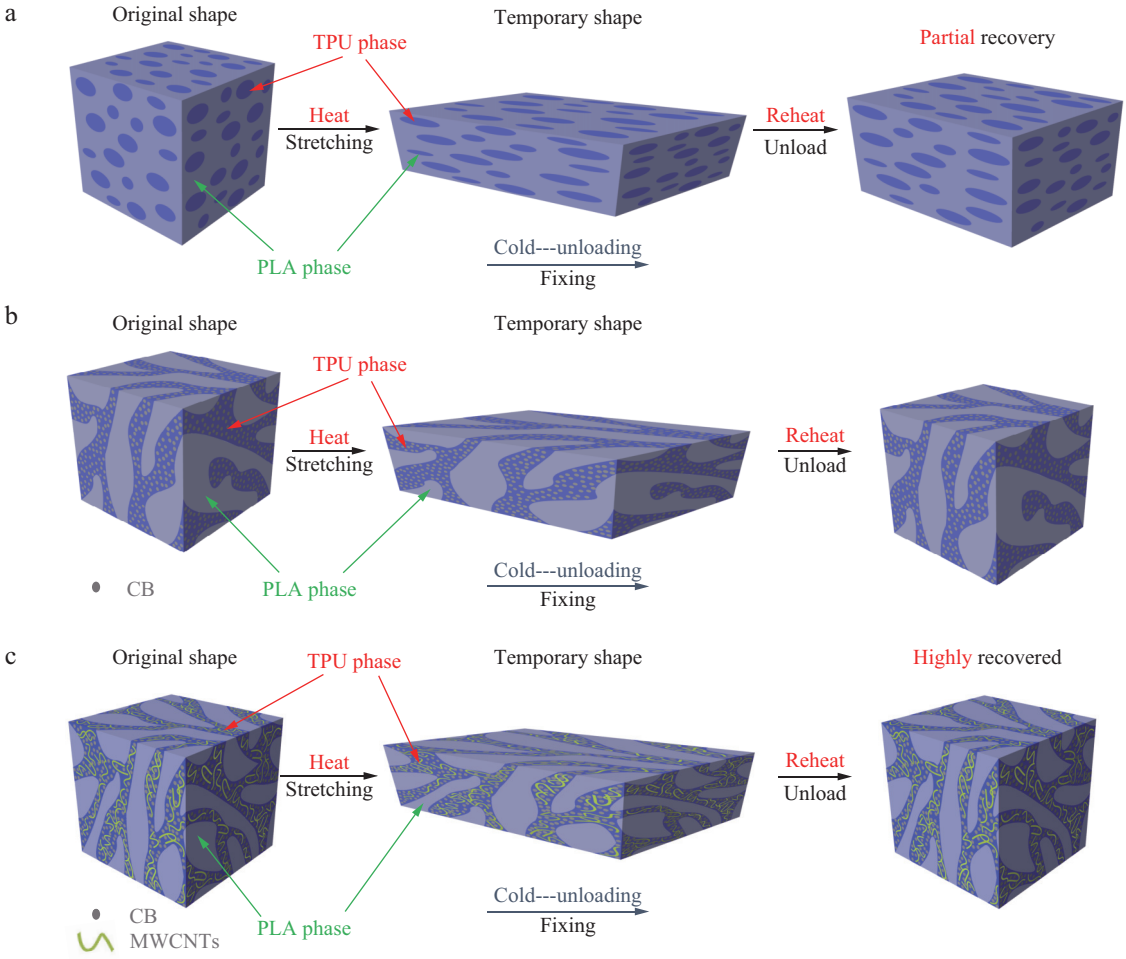

Fig. 7 3D illustration of the shape memory mechanism for (a) PLA70/TPU30, (b) PLA70/TPU30/CB3, and (c) PLA70/TPU30/CB3/CNTs1

continuous structure. CB nanoparticles are capable of self-networking and are selectively located in TPU phase. Then a filler network of CB is formed, which tailors TPU domains to aggregate and fuse together to form such continuous-like phase through their strong affinity. Thus, in such consecutive-like TPU framework, a stronger resilience can be generated, since continuous TPU phase absorbs more energy during deformation. Therefore, PLA70/TPU30/CB3 shows higher R_r than PLA70/TPU30, as shown in Fig. 7(b). During shape recovery, the powerful resilience from deformed TPU plus an intrinsic recovery of deformed PLA chains contribute to such good shape recovery performance together. Interestingly, the incorporated CNTs nanoparticles (1 phr) are also selectively distributed in TPU domains and result in a denser filler network, that is, a more consecutive TPU framework is formed. Therefore, PLA70/TPU30/CB3/CNTs1 shows further increment in R_r due to the higher resilience originated from a more continuous TPU phase, as shown in Fig. 7(c). Nevertheless, the addition of 5 phr CB promotes an even denser filler network than 3 phr CB, which leads to a higher co-continuous degree in PLA70/TPU30/CB5, namely, a higher R_r. However, further introducing 1 phr CNTs impacts very slightly on the continuity of TPU phase since a co-continuous structure of PLA70/TPU30/CB5 has been well-formed already, which explains the negligible differences in R_r between PLA70/TPU30/CB5 and PLA70/TPU30/CB5/CNTs1.

Mechanical Properties of PLA70/TPU30/CB/CNTs

Although SMPs have been used in some fields, the existing limitations still hinder their further applications, for instance, recovery stress at switch temperature (T_s) and inertness to electricity. It is widely accepted that CB and CNTs are not only conductive fillers but also ideal materials to show mechanical reinforcements for polymer materials[30]. In this work, CB and CNTs also act as mechanical reinforcement. Stress-strain tests at T_s (85 °C) of representative composites were conducted on DMA to evaluate their tensile strength at high temperature. Results present a vast increment on tensile stress obtained by filler reinforcements, as shown in Fig. 8. For example, the modulus (stress at 10% strain) of PLA70/TPU30 only equals 0.24 MPa. However, PLA70/TPU30/CB3 and PLA70/TPU30/CB5 exhibit increased moduli of 0.52 and 0.58 MPa, respectively, which shows the value of over 200% due to stiffness CB spheres. Further filled with CNTs, the modulus of PLA70/TPU30/CB3/CNTs1 increases to 0.65 MPa and that of PLA70/ TPU30/CB5/CNTs1 increases to almost 0.91 MPa, nearly 3 and 4

https://doi.org/10.1007/s10118-018-2138-3

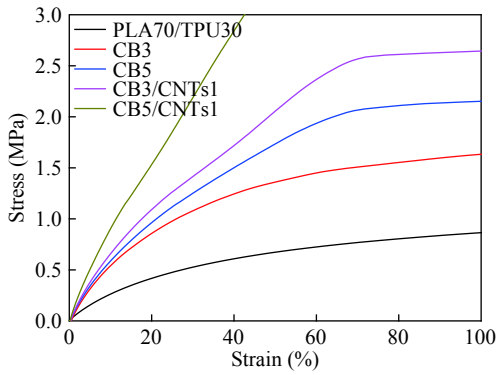

Fig. 8 Tensile test curves (85 °C) of 70PLA/30TPU/CB/CNTs composites

times stronger than PLA70/TPU30, respectively.

Mechanical properties at room temperature of representative composites were also measured, and the tensile strength as well as the notched impact strength of samples are listed in Table 1. It is interesting to find that the notched impact strength of PLA70/TPU30 is vastly improved by CB and CNTs fillers while the tensile strength only changes a little and the Young's modulus of samples remains almost unchanged. Increments in the notched impact strength are believed to be attributed to the morphological evolution of the PLA70/TPU30 blends from the sea-island structure to a co-continuous phase. Thus, the fabricated PLA70/TPU30/CB/CNTs composites which have good stiffness-toughness balance and shape memory performances show great prospects in application such as intelligent devices.

Electrical Conductivity of PLA70/TPU30/CB/CNTs

To achieve electro-actuated SME, the prerequisite is that shape memory polymers exhibit good electrical conductive properties. Based on Joule's law ($Q = U^2t/R$, where Q, U, R, and t represent heat, voltage, electrical resistivity and heating time, respectively), a properly high electrical conductivity or added voltage is required for conductive polymer composites (CPCs) to realize such electrical heating[35, 36]. However, considering the limitation in practical operations especially under hazard circumstances, an electro-actuation by a relatively low voltage shows more advantages. Our previous work shows that PLA70/TPU30/CB6 has the sufficient electrical conductivity to achieve such electro-actuated SME whereas high CB content (6 phr) causes difficulties in fabrication and unfavorable mechanical properties. Thus, it is necessary to reduce the filler content without severely damaging the electrical conductivity. It is widely accepted that CNTs have an inherently electrical conductivity several orders of magnitude higher than CB on the one hand. On the other hand, CNTs can provide a more directly conductive path in polymer due to the high aspect ratio. Herein, CNTs have been introduced in the composites to replace a part of CB, namely, hybrid CB/CNTs fillers are composited into PLA70/TPU30 blend in order to investigate the increment in their electrical conductivities. We aim to seek a proper conductivity which is satisfactory to realize the electro-actuated SME at a relatively low content of filler. Electrical conductive properties of PLA70/TPU30/CB3/CNTs and PLA70/TPU30/CB5/CNTs composites were firstly measured, as plotted in Fig. 9(a).

Results suggest that electrical conductivities of composites

Table 1 Yield strength, Young's modulus, elongation at break and notched impact strength of PLA70/TPU30/CB/CNTs composites

Sample	Yield strength (MPa)	Young's modulus (MPa)	Elongation at break (%)	Notched impact strength (kJ/m^2)
PLA70/TPU30	15.56 ± 0.22	943.10 ± 12.6	365.50 ± 21.10	38.1 ± 0.3
PLA70/TPU30/CB3	15.17 ± 0.91	984.21 ± 30.1	398.27 ± 31.16	53.5 ± 0.5
PLA70/TPU30/CB3/CNTs0.5	18.94 ± 0.49	1088.53 ± 23.6	353.92 ± 29.11	64.2 ± 0.4
PLA70/TPU30/CB3/CNTs1	19.25 ± 0.52	1124.25 ± 7.4	144.24 ± 15.24	65.3 ± 0.4
PLA70/TPU30/CB5	16.88 ± 1.30	937.06 ± 18.9	181.58 ± 36.03	60.4 ± 0.8
PLA70/TPU30/CB5/CNTs0.5	19.09 ± 0.48	927.79 ± 24.5	138.94 ± 37.20	66.7 ± 0.6
PLA70/TPU30/CB/CNTs1	22.42 ± 0.43	1015.88 ± 13.8	112.82 ± 14.02	66.7 ± 0.5

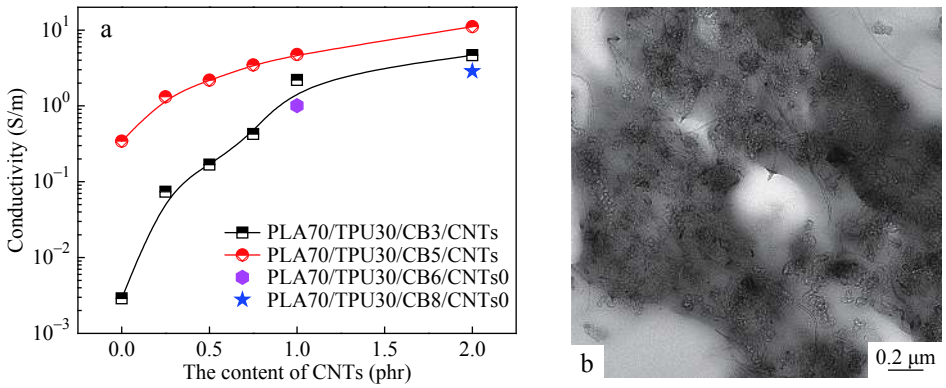

Fig. 9 (a) Electrical conductivity of PLA70/TPU30/CB3 and PLA70/TPU30/CB5 filled with different contents of CNTs. The magenta hexagon and blue star show the electrical conductivity of PLA70/TPU30/CB6/CNTs0 and PLA70/TPU30/CB8/CNTs0 composites for comparison, respectively. (b) High amplification TEM images of PLA70/TPU30/CB3/CNTs1

https://doi.org/10.1007/s10118-018-2138-3

with the same content of CB are tremendously increased along with the addition of CNTs. The electrical conductivity of PLA70/TPU30/CB3 is 2.9 × 10^{-3} S/m, while that of PLA70/TPU30/CB3/CNTs1 increases to 2.2 S/m, exhibiting enhancement of three orders of magnitude. Furthermore, the electrical conductivity of PLA70/TPU30/CB5 increases from 0.342 S/m to 4.76 S/m after the addition of 1 phr CNTs. It is notable that the conductivity of PLA70/TPU30/CB3/CNTs1 is higher than that of PLA70/TPU30/CB6 (1.01 S/m), and it is comparable to PLA70/TPU30/CB8 (2.87 S/m). Therefore, it is feasible to introduce a small content of CNTs to replace some CB, in order to improve the preparation of composites while obtaining an excellent electrical conductivity.

Such results should be attributed to at least two reasons. (1) Double percolation conductive network of CNTs and CB has formed in polymer matrix. (2) Combined effect of CNTs and CB improves the conductive pathway and reduces the redundancy of conductive network[30]. Both can be explained through filler network. Selectively localized CB (in TPU phase) constructs a filler network, which becomes denser when more CB is introduced. Percolated CB network tailors discrete TPU domains into continuous phase through their affinity as discussed above, and provides relatively good electrical conductivity for the polymer matrix. However, according to the electron pass mechanism in CPCs, electrons are transported through conductively filler networks *via* direct contact or tunneling effect[37]. Spherical CB nanoparticles are considered to be difficult to contact with each other, thus more electrons are passed by tunneling, resulting in poor inherent electrical conductivity. Therefore, an extremely high network density is required to achieve relatively high electrical conductivity, namely, high content of CB is required to achieve electro-actuated SME, which is unfavorable to processing or mechanical properties. However, CNTs form more direct and efficient conductive network in the polymer matrix *via* bridging each other due to its high aspect ratio, and electrons prefer to transport through CNTs directly. CNTs' higher inherent conductivity also improves CPCs' conductive properties. Herein, CB nanoparticles act as link-points which connect discontinuous CNTs conductive pathways and reduce the redundancy of conductive network, which further decreases the resistance. Nevertheless, TEM observation confirms that CB and CNTs connect with each other and form more efficient conductive path (Fig. 9b), ensuring high electrical conductivity at a relatively low hybrid filler content.

Electro-actuated SME of PLA70/TPU30/CB/CNTs

A high electrical conductivity is believed to be helpful to the electro-actuated SME, since more Joule's heat can be generated by the same voltage in unit time. The surface temperature of representative composites under voltage of 30 V was firstly evaluated and results are demonstrated in Fig. 10. Results for tested surface temperature versus time under 30 V of samples are plotted in Fig. 10(a), while the

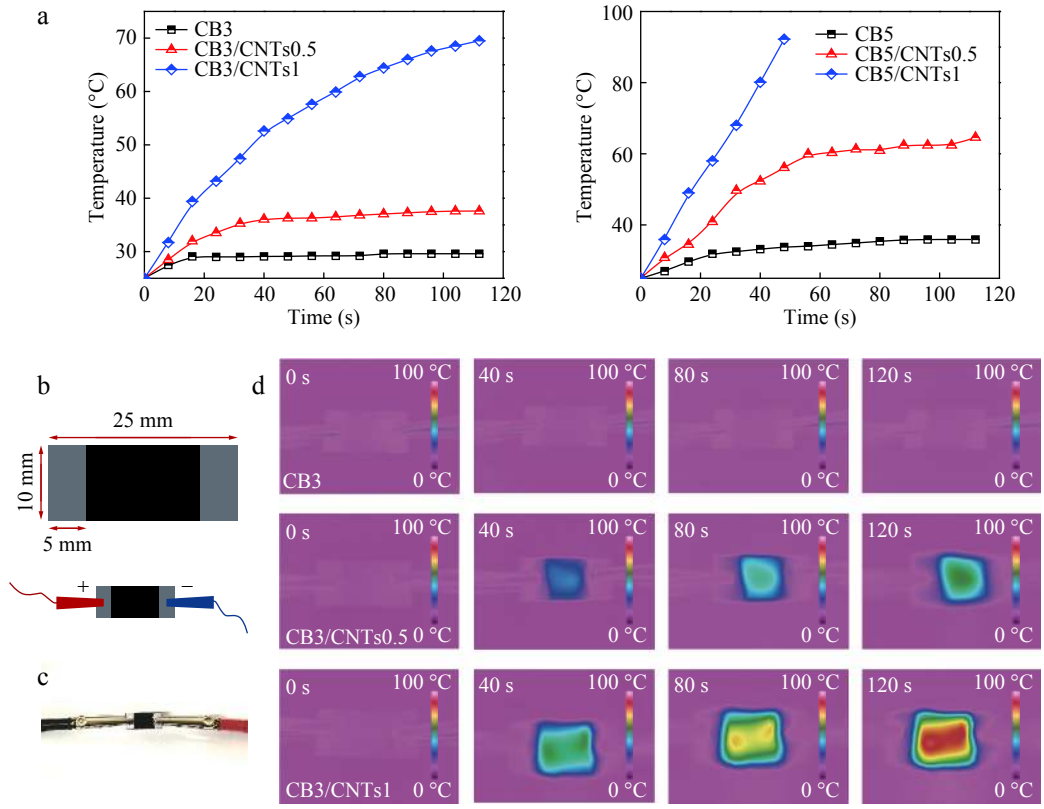

Fig. 10 (a) Surface temperature as a functuon of time of PLA70/TPU30/CB/CNTs composites under voltage of 30 V; (b) Sample preparation schematics, grey part indicates silver coating; (c) Sample testing methods, grey part indicates silver coating; (d) IR-thermal images of PLA70/TPU30/CB3/CNTs composites as a funtion of time under voltage of 30 V (The online version is colorful.)

https://doi.org/10.1007/s10118-018-2138-3

preparation and testing schematics of samples are shown in Figs. 10(b) and 10(c). Fig. 10(d) shows the infrared photos of the surface temperature of PLA70/TPU30/CB3/CNTs under 30 V. Results show that PLA70/TPU30/CB3 is unable to be stimulated at 30 V due to its relatively low electrical conductivity, while PLA70/TPU30/CB3/CNTs0.5 can be heated to about 50 °C in 100 s. Moreover, PLA70/TPU30/CB3/CNTs1 can be heated to almost 100 °C in 120 s, suggesting that the addition of CNTs tremendously improves the electrical conductivities of composites. Despite the fact that PLA70/TPU30/CB5 exhibits almost inertness to 30 V by only reaching about 37 °C, PLA70/TPU30/CB5/CNTs0.5 retains at 60 °C in 100 s, and PLA70/TPU30/CB5/CNTs1 can be rapidly heated to 100 °C within only 50 s. Infrared photographs further illustrate the changes in surface temperature of PLA70/TPU30/CB3/CNTs composites at 30 V. PLA70/TPU30/CB3 shows no apparent surface temperature change at 30 V, while the center surface of PLA70/TPU30/CB3/CNTs1 is heated to almost 100 °C in 120 s. Obviously, the sample with a higher electrical conductivity gets faster surface temperature climbing beneath 30 V because a more conductive sample obtains more Joule's heat in unit time. The hybrid CB/CNTs conductive network provides excellent electrical properties to achieve electro-actuation on the one hand. On the other hand, the filler network is also capable to supply the morphological evolution of TPU phase and finally results in such good shape memory properties. Thus, adding a small content of CNTs to replace some CB is considered to be efficient to improve the electrical conductivity of composites while lowering the content of fillers.

The electro-actuated SME of representative composites was investigated through a bending test method, experimently, where the details and results are displayed in Fig. 11. Shape recovery ratio with the escaping time of tested samples under the voltage of 30 V is shown in Fig. 11(a), and comparsion is made between PLA70/TPU30/CB/CNTs and PLA70/TPU30/CB composites. Fig. 11(b) shows the preparation and testing schematics of the tested samples. One should be noted that no detectable recovery occurred after fixity. The electro-actuated SME is intiated by loading 30 V, and the specimen gradually recovers from the "U" shape to its permanent shape (flat). The electro-actuated recovery process of PLA70/TPU30/CB3/CNTs1 is displayed in Fig. 11(c) and the infrared images of electro-actuating recovery process of this composite are illustrated in Fig. 11(d). The whole electro-actuated shape recovery process can be divided into 3 stages. Firstly, the recovery progress is relatively slower (named first stage). This phenomenon is most apparent to PLA70/TPU30/CB6, which shows a relatively low recovery rate (~0.3 %/s) in the first 50 s. For the other three tested samples, it is seemed that the first stage becomes shorter with higher recovery rate. PLA70/TPU30/CB8 and PLA70/TPU30/CB3/CNTs1 exhibit about 40 s long for the first stage with a rate of about 0.5 %/s. And PLA70/TPU30/CB5/CNTs1 takes only about 10 s to complete the first stage at the speed of 1.5 %/s. The difference in the first stage is considered to result from the different electrical conductivity. It seems that the samples have started shape recovery before heated to T_s, which is

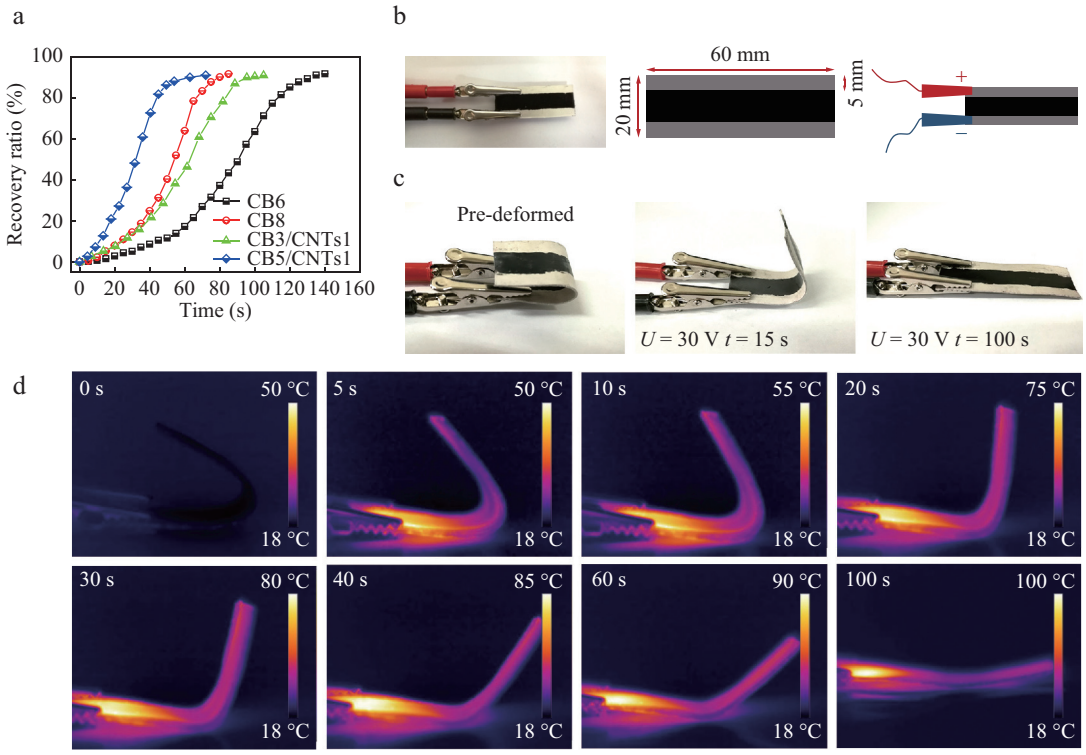

Fig. 11 (a) Time dependence shape recovery ratio of the PLA70/TPU30/CB/CNTs composites; (b) Preparation of eletro-actuated shape behavior tests; (c) Shape recovery process of PLA70/TPU30/CB3/CNTs1; (d) Infrared images of shape recovery process of PLA70/TPU30/CB3/CNTs1 (The online version is colorful.)

https://doi.org/10.1007/s10118-018-2138-3

confirmed by infrared photogrphy in Fig. 11(d). Some PLA molecular chains have been unfrozen in advance with increasing temperature, but the recovery speed remains at a low rate due to the residual restriction from those glassy PLA domains. The sample which has a relatively high electrical conductivity is heated to T_s faster, resulting in the shorter first stage. Moreover, a higher filler content provides a higher degree of morphological co-continuity and more mechanical reinforments, so these samples possess higher resilience and exhibit faster recovery. The second stage exhibits the fastest recovery. Obviously, when samples are heated upon T_s, the recovery speed reaches the maximum since all molecular restrictions have been removed. PLA70/TPU30/CB8 and PLA70/TPU30/CB5/CNTs1 show similar recovery speed (~3 %/s), which is faster than PLA70/TPU30/CB3/CNTs1 (~1.75 %/s), while PLA70/TPU30/CB6 exhibits the slowest recovery (about 1 %/s). The recovery rate in the second stage is also considered to be benefited from resilience affected by the morphological co-continuity as well as the filler reinforcements, and this stage ends when R_r reaches about 80%. The last stage of recovery (named third stage) shows a vastly decreased recovery speed (<0.4 %/s), which suggests that the stored stress has almost been released during the first and second stages. As a result, the third stage shows the slowest recovery in about 20 s to complete shape recovery.

Four composites all show a R_r of about 90%, as calculated from Eq. (3). PLA70/TPU30/CB5/CNTs1 exhibits the fastest recovery performance due to the highest electrical conductivity, completing full recovery in 70 s. PLA70/TPU30/CB3/CNTs1 completes recovery in 100 with the value between PLA70/TPU30/CB8 and PLA70/TPU30/CB6 which consume 80 and 140 s, respectively. However, PLA70/ TPU30/CB3 and PLA70/TPU30/CB5 (not shown in Fig. 11) are considered to not equip such electro-actuated SME at 30 V due to their relatively low electrical conductivity, as aforementioned. Thus, it is believed that adding 1 phr CNTs can tremendously improve electrical conductivity *via* more efficient and integrated conductive network, which improves the electro-actuated SME of composites.

Generally speaking, achieving the electro-actuated SMPs with a high electrical conductivity through the additon of a high content of CB will cause unfavourable mechanical properties and difficulties in fabrication. In this work, PLA70/TPU30/CB3/CNTs1 shows the faster electro-induced recovery and a higher R_r at a relatively lower filler content (4 phr in total) than PLA70/TPU30/CB6 in our previous work (6 phr in total). Therefore, introducing a small content of CNTs to replace some CB is considered to be efficient to improve the electro-actuated shape memory performances as well as the mechanical properties of composites at a lower content of filler.

CONCLUSIONS

In this work, hybrid CB/CNTs fillers were introduced into PLA/TPU blends (70/30 by weight) in order to decrease the content of filler and improve the electrical conductivity of PLA70/TPU30/CB composites based on our recent work. Related properties which are affected by the addition of CNTs such as shape memory behaviors and mechanical properties were also investigated. Both CB and CNTs nanoparticles are selectively located in TPU, assembling a denser filler network *via* self-networking and facilitating the morphological evolution of PLA70/TPU30 blends from the sea-island structure to a unique co-continuous structure, which results in a higher continuity of TPU phase. Such increment in co-continuity also improves the mechanical properties as well as the shape memory behavior. Moreover, hybrid CB/CNTs fillers are selectively distributed in the continuous TPU phase which results in better electrical conductivity due to the double percolation conductive network. Nevertheless, CNTs nanoparticles form a more efficient electrical conductive network due to the higher inherent conductivity and high aspect ratio, while the presence of CNTs most likely links the dispersed CB nanoparticles, which tremendously decreases the redundancy of the conductive network and promotes a superior electrical conductivity. PLA70/TPU30/CB3/CNTs1 shows a rapid electro-actuated SME, recovering to original shape within 100 s at 30 V. Our work further improves the strategy to fabricate plastic/elastomer/fillers composites with well-balanced shape memory properties and superior electrical conductivities at lower filler content. Moreover, such composites show a mechanical property of balanced stiffness-toughness as well as simple fabrication, which is very important in industrial productions and applications, such as soft robotics and artificial mussels.

ACKNOWLEDGMENTS

This work was financially supported by the National Natural Science Foundation of China (Nos. 51421061 and 51210005).

REFERENCES

1 Lendlein, A.; Kelch, S. Shape-memory polymers. Angew. Chem. Int. Ed. 2002, 41(12), 2034.
2 Hu, J. L.; Zhu, Y.; Huang, H. H.; Lu, J. Recent advances in shape-memory polymers, structure; mechanism; functionality; modeling and applications. Prog. Polym. Sci. 2012, 37(12), 1720−1763.
3 Zhao, Q.; Qi, H. J.; Xie, T. Recent progress in shape memory polymer, new behavior; enabling materials; and mechanistic understanding. Prog. Polym. Sci. 2015, 49-50, 79−120.
4 Xie, T. Recent advances in polymer shape memory. Polymer 2011, 52(22), 4985−5000.
5 Liu, Y. J.; Lv, H. B.; Lan, X.; Leng, J.; Du, S. Y. Review of electro-active shape-memory polymer composite. Compos. Sci. Technol. 2009, 69(13), 2064−2068.
6 Tang, Z. H.; Sun, D. Q.; Yang, D.; Guo, B. C.; Zhang, L. Q.; Jia, D. M. Vapor grown carbon nanofiber reinforced bio-based polyester for electroactive shape memory performance. Compos. Sci. Technol. 2013, 75, 15−21.
7 Zhang, Z. X.; Wang, W. Y.; Yang, J. H.; Zhang, N.; Huang, T.; Wang, Y. Excellent electroactive shape memory performance of EVA/PCL/CNT blend composites with selectively localized CNTs. J. Phys. Chem. C 2016, 120(40), 22793−22802.
8 Xiao, Y.; Zhou, S.; Wang, L.; Gong T. Electro-active shape memory properties of poly(epsilon-caprolactone)/ functionalized multiwalled carbon nanotube nanocomposite.

ACS Appl. Mater. Interfaces 2012, 2(12), 3506−3514.
9 Leng, J. S.; Huang, W. M.; Lan, X.; Liu, Y. J.; Du, S. Y. Significantly reducing electrical resistivity by forming conductive Ni chains in a polyurethane shape-memory polymer/carbon-black composite. Appl. Phys. Lett. 2008, 92(20), 204101.
10 Yu, K.; Zhang, Z. C.; Liu, Y. J.; Leng J. S. Carbon nanotube chains in a shape memory polymer/carbon black composite, to significantly reduce the electrical resistivity. Appl. Phys. Lett. 2011, 98(7), 074102.
11 Wang, X.; Zhao, J.; Chen, M.; Ma, L.; Zhao, X.; Dang, Z. M. Improved self-healing of polyethylene/carbon black nanocomposites by their shape memory effect. J. Phys. Chem. B 2013, 117(5), 1467−1474.
12 Wang, X.; Sparkman, J.; Gou J. H. Electrical actuation and shape memory behavior of polyurethane composites incorporated with printed carbon nanotube layers. Compos. Sci. Technol. 2017, 141, 8−15.
13 Wang, K.; Zhu, G. M.; Yan, X. G.; Ren, F.; Cui, X. P. Electroactive shape memory cyanate/polybutadiene epoxy composites filled with carbon black. Chinese J. Polym. Sci. 2016, 34(4), 466−474.
14 Guo, Y. L.; Zhang, R. Z.; Wu, K.; Chen, F.; Fu, Q. Preparation of nylon MXD6/EG/CNTs ternary composites with excellent thermal conductivity and electromagnetic interference shielding effectiveness. Chinese J. Polym. Sci. 2017, 35(12), 1497−1507.
15 Meng, H.; Li, G. Q. A review of stimuli-responsive shape memory polymer composites. Polymer 2013, 54(9), 2199−2221.
16 Meng, Q.; Hu, J. A review of shape memory polymer composites and blends. Compos. Part A Appl. Sci. Manuf. 2009, 40(11), 1661−1672.
17 You, J. C.; Dong, W. Y.; Zhao, L. P.; Cao, X. J.; Qiu, J. S.; Sheng, W. J.; Li, Y. J. Crystal orientation behavior and shape-memory performance of poly(vinylidene fluoride)/acrylic copolymer blends. J. Phys. Chem. B 2012, 116(4), 1256−1264.
18 You, J. C.; Fu, H.; Dong, W. Y.; Zhao, L. P.; Cao, X. J.; Li, Y. J. Shape memory performance of thermoplastic polyvinylidene fluoride/acrylic copolymer blends physically cross-linked by tiny crystals. ACS Appl. Mater. Interfaces 2012, 4(9), 4825−4831.
19 Zhang, H.; Wang, H. T.; Zhong, W.; Du, Q. G. A novel type of shape memory polymer blend and the shape memory mechanism. Polymer 2009, 50(6), 1596−1601.
20 Kurahashi, E.; Sugimoto, H.; Nakanishi, E.; Nagata, K.; Inomata, K. Shape memory properties of polyurethane/poly(oxyethylene) blends. Soft Matter 2012, 8(2), 496−503.
21 Yuan, D. S.; Chen, Z. H.; Xu, C. H.; Chen, K. L.; Chen Y. K. Fully biobased shape memory material based on novel cocontinuous structure in poly(lactic acid)/natural rubber TPVs fabricated *via* peroxide-induced dynamic vulcanization and in situ interfacial compatibilization. ACS Sustain. Chem. Eng. 2015, 3(11), 2856−2865.
22 Zheng, Y.; Dong, R. Q.; Shen, J. B.; Guo, S. Y. Tunable shape memory performances *via* multilayer assembly of thermoplastic polyurethane and polycaprolactone. ACS Appl. Mater. Interfaces 2016, 8(2), 1371−1380.
23 Gubbels, F.; Blacher, S.; Vanlathem, E.; Jerome, R.; Deltour, R.; Brouers, F.; Teyssie, P. Design of electrical composites, determining the role of the morphology on the electrical properties of carbon black filled polymer blends. Macromolecules 1995, 28(5), 1559−1566.
24 Wu, G.; Li, B.; Jiang, J. Carbon black self-networking induced co-continuity of immiscible polymer blends. Polymer 2010, 51(9), 2077−2083.
25 Xiu, H.; Huang, C. M.; Bai, H. W.; Jiang, J.; Chen, F.; Deng, H.; Zhang, Q.; Fu, Q. Improving impact toughness of polylactide/poly(ether)urethane blends *via* designing the phase morphology assisted by hydrophilic silica nanoparticles. Polymer 2014, 55(6), 1593−1600.
26 Xiu, H.; Zhou, Y.; Huang, C. M.; Bai, H. W.; Zhang, Q.; Fu, Q. Deep insight into the key role of carbon black self-networking in the formation of co-continuous-like morphology in polylactide/poly(ether)urethane blends. Polymer 2016, 82, 11−21.
27 Odent, J.; Habibi, Y.; Raquez, J. M.; Dubois, P. Ultra-tough polylactide-based materials synergistically designed in the presence of rubbery ε-caprolactone-based copolyester and silica nanoparticles. Compos. Sci. Technol. 2013, 84, 86−91.
28 Qi, X. D.; Xiu, H.; Wei, Y.; Zhou, Y.; Guo, Y. L.; Huang, R.; Bai, H. W.; Fu, Q. Enhanced shape memory property of polylactide/thermoplastic poly(ether)urethane composites *via* carbon black self-networking induced co-continuous structure. Compos. Sci. Technol. 2017, 139, 8−16.
29 Sun, Y.; Bao, H. D.; Guo, Z. X.; Yu, J. Modeling of the electrical percolation of mixed carbon fillers in polymer-based composites. Macromolecules 2009, 42(1), 459−463.
30 Ma, P. C.; Liu, M. Y.; Zhang, H.; Wang, S. Q.; Wang, R.; Wang, K.; Wong, Y. K.; Tang, B. Z.; Hong, S. H.; Paik, K. W.; Kim, J. K. Enhanced electrical conductivity of nanocomposites containing hybrid fillers of carbon nanotubes and carbon black. ACS Appl. Mater. Interfaces 2009, 1(5), 1090−1096.
31 Chen, J.; Du, X. C.; Zhang, W. B.; Yang, J. H.; Zhang, N.; Huang, T.; Wang; Y. Synergistic effect of carbon nanotubes and carbon black on electrical conductivity of PA6/ABS blend. Compos. Sci. Technol. 2013, 81, 1−8.
32 Zou, H.; Wang, K.; Zhang, Q.; Fu, Q. A change of phase morphology in poly(*p*-phenylene sulfide)/polyamide 66 blends induced by adding multi-walled carbon nanotubes. Polymer 2006, 47(22), 7821−7826.
33 Shi. Y. Y; Zhang, W. B.; Yang J. H.; Huang, T.; Zhang, N.; Wang, Y.; Yuan, G. P.; Zhang, C. L. Super toughening of the poly(L-lactide)/thermoplastic polyurethane blends by carbon nanotubes. RSC Adv. 2013, 3(48), 26271−26282.
34 Xiao, Y. J.; Wang W. Y.; Lin, T.; Chen, X. J.; Zhang, Y. T.; Yang J. H.; Wang, Y.; Zhou, Z. W. Largely enhanced thermal conductivity and high dielectric constant of poly(vinylidene fluoride)/boron nitride composites achieved by adding a few Carbon Nanotubes. J. Phys. Chem. C 2016, 120(12), 6344−6355.
35 He, M. J.; Xiao, W. X.; Xie, H.; Fan, C. J.; Du, L.; Deng, X. Y.; Wang, Y. Z. Facile fabrication of ternary nanocomposites with selective dispersion of multi-walled carbon nanotubes to access multi-stimuli-responsive shape-memory effects. Mater. Chem. Front. 2017, 1, 343−353.
36 Tang, Z. H.; Kang, H. L.; Wei, Q. Y.; Guo, B. C.; Zhang, L. Q.; Jia, D. M. Incorporation of graphene into polyester/carbon nanofibers composites for better multi-stimuli responsive shape memory performances. Carbon 2013, 64, 487−498.
37 Xu, Z. H.; Zhang, Y. Q.; Wang, Z. G.; Sun, N.; Li, H. Enhancement of electrical conductivity by changing phase morphology for composites consisting of polylactide and poly(epsilon-caprolactone) filled with acid-oxidized multiwalled carbon nanotubes. ACS Appl. Mater. Interfaces 2011, 3(12), 4858−4864.

https://doi.org/10.1007/s10118-018-2138-3